Available online at www.sciencedirect.com
ScienceDirect
Journal of Computational Physics 227 (2008) 2886–2898
JOURNAL OF COMPUTATIONAL PHYSICS
www.elsevier.com/locate/jcp

# Stability criteria for hybrid difference methods

Johan Larsson [a,*], Bertil Gustafsson [a,b]

[a] Center for Turbulence Research, Stanford University, Stanford, CA 94305, United States
[b] Department of Information Technology, Scientific Computing, Uppsala University, P.O. Box 337, S-75105 Uppsala, Sweden

Received 17 June 2007; received in revised form 20 September 2007; accepted 16 November 2007
Available online 2 January 2008

**Abstract**

The stability of hybrid difference methods, where different schemes are used in different parts of the domain, is examined for general schemes. It is shown that the energy method with the natural norm does not prove stability, but that the Kreiss or 'GKS' theory yields sufficient criteria for stability. While the analysis is general, it is discussed primarily in the context of hybrid schemes for shock/turbulence interactions, where a robust shock-capturing scheme is used around the discontinuities and an efficient linear scheme is used in other regions. An example of two coupled schemes that are individually stable yet unstable when coupled is given, showing that stability of hybrid methods is an important and non-trivial matter.


*Keywords:* Stability; Numerical analysis; Difference methods; Kreiss; Interface; Hybrid

## 1. Introduction

Hybrid numerical methods are becoming increasingly popular for problems where different physics are important in different parts of the domain. The hybridization can take many different forms, some examples of which include: the coupling of different codes to solve different underlying PDEs in different regions (say, the compressible and incompressible Navier–Stokes equations); the use of grids with different topologies in different regions (say, structured and unstructured grids); and the use of different numerical schemes in different regions within the same code and PDE. The latter situation arises in the computation of flows with shock waves, density interfaces, and turbulence, where one might use a computationally efficient and accurate linear scheme in the turbulence regions and a more robust nonlinear shock-capturing scheme around the discontinuities. These hybrid methods are typically implemented by using one scheme for $x \leqslant 0$ and the other for $x > 0$, say, where the interface location may depend on the instantaneous solution.

Ideally, a hybrid method combines the strengths of the individual methods being used, but accuracy and stability at the interface between the schemes is an issue that must be resolved. Even when both schemes are stable individually, there is no guarantee that the coupled method will be stable. One common class of hybrid methods couples an ENO or WENO scheme [1] with a centered or upwinded linear scheme. Adams

* Corresponding author. Tel.: +1 650 723 9286.
*E-mail address:* jola@stanford.edu (J. Larsson).

0021-9991/$ - see front matter © 2007 Elsevier Inc. All rights reserved.
doi:10.1016/j.jcp.2007.11.025

and Shariff [2] used the combination ENO/upwinded Padé and noticed small oscillations (noise) around the interface. Later, Ren et al. [3] argued that the sharp transition from one scheme to the other is responsible for the noise, and proposed an approach where the schemes are smoothly blended into each other over several grid points. Hill and Pullin [4] argued that the noise around the interface can be minimized by forcing the optimal WENO stencil to equal that of the linear scheme, thus avoiding or minimizing the change across the interface.

In this paper, we analyze the stability characteristics of a general hybrid method using a linear model problem. The hybrid method is considered to consist of two arbitrary but different and linear consistent schemes. Thus the analysis applies for problems where both the PDE and the potentially nonlinear shock-capturing scheme are linearized.

The model problem will be defined in Section 2, and it will be shown that the energy method together with the most natural choice of norm can not be used to prove stability. This does not imply that the energy method categorically fails for this problem, since there are infinitely many energy norms that one could consider.

Thus we instead turn to the Kreiss theory [5,6] (sometimes referred to as 'GKS' theory) and give criteria for which the Kreiss condition is satisfied, thus proving stability. Strikwerda [7] showed that the Kreiss condition leads to stability in the generalized sense for semi-discrete problems. In [6] it was shown that strong stability follows from the Kreiss condition under certain restrictions. The present analysis is somewhat similar to Goldberg and Tadmor [8], who used the Kreiss theory to prove stability of hyperbolic initial-boundary value problems for rather general schemes and boundary conditions. Ciment [9] analyzed a similar coupled problem where both schemes are dissipative.

A few examples will be discussed, including one involving two schemes that are individually stable yet unstable when coupled. This illustrates that stability of hybrid methods is both an important and non-trivial matter.

## 2. Problem definition

Consider the hyperbolic half-space problem

$$u_t + u_x = 0, \quad -\infty < x < \infty, \quad t \geqslant 0. \tag{1}$$

Note that while a scalar problem is analyzed here, the analysis applies equally to hyperbolic systems of form

$$q_t + A q_x = 0, \quad -\infty < x < \infty, \quad t \geqslant 0,$$

where $A$ is a diagonalizable matrix. For such systems, the scalar model problem (1) represents each component of the diagonalized system (cf. [8]).

To facilitate later discretization using different schemes coupled at $x = 0$, the model problem can equivalently be written on the folded form

$$\begin{aligned} &u_t^{\mathrm{I}} = u_x^{\mathrm{I}}, \quad x \geqslant 0, \\ &u_t^{\mathrm{II}} = -u_x^{\mathrm{II}}, \quad x \geqslant 0, \\ &u^{\mathrm{I}}(0,t) = u^{\mathrm{II}}(0,t), \end{aligned}$$

where

$$u(x,t) = \begin{cases} u^{\mathrm{I}}(-x,t), & x \leqslant 0. \\ u^{\mathrm{II}}(x,t), & x > 0. \end{cases} \tag{2}$$

A sketch of the original and folded forms of the model problem is shown in Fig. 1. Discretization in space yields

$$\frac{\mathrm{d}u_j^{\mathrm{I}}}{\mathrm{d}t} = \frac{1}{h} \sum_{k=-l_{\mathrm{I}}}^{r_{\mathrm{I}}} a_k^{\mathrm{I}} u_{j+k}^{\mathrm{I}}, \quad j = 0, 1, \ldots, \tag{3a}$$

$$\frac{\mathrm{d}u_j^{\mathrm{II}}}{\mathrm{d}t} = -\frac{1}{h} \sum_{k=-l_{\mathrm{II}}}^{r_{\mathrm{II}}} a_k^{\mathrm{II}} u_{j+k}^{\mathrm{II}}, \quad j = 1, 2, \ldots, \tag{3b}$$

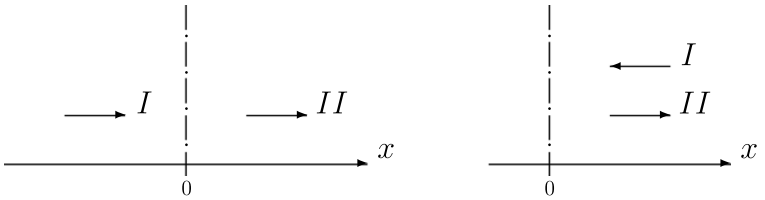


Fig. 1. Sketch of the model problem in original (left) and folded (right) forms. The arrows and symbols indicate flow direction and scheme.

where $\{a_k^{\mathrm{I,II}}\}$ are the coefficients of the individual schemes, $u_j^{\mathrm{I,II}}(t)$ approximates $u^{\mathrm{I,II}}(hj,t)$, and $h$ is the uniform grid spacing. The boundary conditions are

$$u_j^{\mathrm{I}} = u_{-j}^{\mathrm{II}}, \quad j = -l_{\mathrm{I}}, \ldots, l_{\mathrm{II}} - 1. \tag{4}$$

The schemes are required to be consistent and the coefficients must satisfy

$$\sum_{k=-l_{\mathrm{I,II}}}^{r_{\mathrm{I,II}}} a_k^{\mathrm{I,II}} = 0, \tag{5a}$$

$$\sum_{k=-l_{\mathrm{I,II}}}^{r_{\mathrm{I,II}}} k a_k^{\mathrm{I,II}} = 1. \tag{5b}$$

One should note that, due to the opposite directions of the characteristics in the folded problem, the operation of switching schemes corresponds to the transformation $a_k^{\mathrm{I}} \to -a_{-k}^{\mathrm{II}}, a_k^{\mathrm{II}} \to -a_{-k}^{\mathrm{I}}$ (easily seen by splitting the coefficients into symmetric and anti-symmetric parts). The inner product of two real functions $u$ and $v$ is defined as

$$(u,v) = (u^{\mathrm{I}}, v^{\mathrm{I}})_{\mathrm{I}} + (u^{\mathrm{II}}, v^{\mathrm{II}})_{\mathrm{II}} = h\sum_{j=0}^{\infty} u_j^{\mathrm{I}} v_j^{\mathrm{I}} + h\sum_{j=1}^{\infty} u_j^{\mathrm{II}} v_j^{\mathrm{II}}, \tag{6}$$

with the norm $\|u\|^2 = (u,u)$. Naturally, only solutions which satisfy $\|u\| < \infty$ are of interest.

### 2.1. The energy method

The natural norm defined in (6) is the perhaps most obvious choice of norm for a coupled problem, since the interface is located in the interior of the domain. To show that the energy method can not be used to prove stability in this norm, consider the specific combination $(a_{-1}^{\mathrm{I}}, a_0^{\mathrm{I}}, a_1^{\mathrm{I}}) = (-1/2, 0, 1/2)$ and $(a_{-1}^{\mathrm{II}}, a_0^{\mathrm{II}}, a_1^{\mathrm{II}}) = (-1/2 - \alpha, 2\alpha, 1/2 - \alpha)$ with $l_{\mathrm{I,II}} = r_{\mathrm{I,II}} = 1$. This corresponds to using a central scheme everywhere, but with a dissipation term (with coefficient $\alpha h > 0$) turned on suddenly for $j > 0$. Taking the inner product $(u, u_t)$ using (3) yields

$$(u,u_t) = -\frac{1}{2}u_0^{\mathrm{I}}u_{-1}^{\mathrm{I}} + \left(\alpha + \frac{1}{2}\right)u_0^{\mathrm{II}}u_1^{\mathrm{II}} + 2\alpha\sum_{j=1}^{\infty} u_j^{\mathrm{II}}\left(u_{j+1}^{\mathrm{II}} - u_j^{\mathrm{II}}\right),$$

which with the boundary conditions becomes

$$\frac{\mathrm{d}\|u\|^2}{\mathrm{d}t} = 2\alpha u_0^{\mathrm{II}}u_1^{\mathrm{II}} + 4\alpha\sum_{j=1}^{\infty} u_j^{\mathrm{II}}\left(u_{j+1}^{\mathrm{II}} - u_j^{\mathrm{II}}\right).$$

For stability one would require the norm growth rate to be bounded independently of the grid spacing $h$, i.e. $\|u\|_t^2 \leqslant C\|u\|^2$ for some constant $C$. However, it is trivial to find grid functions $u_j$ (where $u_j$ is defined in analogy with (2)) where this is not the case. Take for example $(u_0^{\mathrm{II}}, u_1^{\mathrm{II}}) = (1, 1/4)$ and all remaining values equal to zero. This yields

$$\frac{\mathrm{d}\|u\|^2}{\mathrm{d}t} = \frac{\alpha}{4},$$
$$\|u\|^2 = \frac{17h}{16},$$

and hence the energy estimate must have $C \to \infty$ as $h \to 0$. Interestingly, the energy growth rate for this particular grid function increases with increasing dissipation.

The energy method with the natural norm shows that there are solutions that grow over short times (in this norm), but this does not imply that the method is unstable. This situation is common with the energy method and is related to the fact that it, essentially, considers the symmetric part of the discretization matrix only, rather than the matrix itself. The example provided here yields a discretization that is neither symmetric nor anti-symmetric close to the interface, and is such that the symmetric part has eigenvalues with positive real part despite the method actually being stable.

For the simple example used here, a norm with different weights for the I and II parts could most likely be used to prove stability, but for more complex and general schemes it is not trivial to find the appropriate norm. The Kreiss theory [5,6] does not have this drawback.

## 3. The Kreiss theory

The Kreiss theory [5,6] finds an energy estimate by use of Laplace transforms in time, and hence it considers normal modes of form $u_j^{\mathrm{I}} = \hat{u}_j \exp(st)$ and $u_j^{\mathrm{II}} = \hat{v}_j \exp(st)$. Inserting into (3) yields two constant-coefficient difference equations with solutions of form $\hat{u}_j \sim \kappa^j$ and $\hat{v}_j \sim \mu^j$ where $\kappa$ and $\mu$ are roots of the characteristic equations (cf. [6])

$$\tilde{s} = \sum_{k=-l_{\mathrm{I}}}^{r_{\mathrm{I}}} a_k^{\mathrm{I}} \kappa^k, \tag{7a}$$

$$\tilde{s} = -\sum_{k=-l_{\mathrm{II}}}^{r_{\mathrm{II}}} a_k^{\mathrm{II}} \mu^k, \tag{7b}$$

where $\tilde{s} = sh$. Stability is ensured if the Kreiss condition is satisfied, which amounts to verifying that there is no combination of $\tilde{s}$, $\kappa$, and $\mu$ that satisfies the characteristic equations and the boundary conditions for $\mathrm{Re}\,\tilde{s} \geqslant 0$. One important but subtle point in the Kreiss theory is that the line $\mathrm{Re}\,\tilde{s} = 0$ (in the complex plane) is investigated as the limit $\mathrm{Re}\,\tilde{s} \to 0^+$ (from the right half-plane). Thus conditions at $\mathrm{Re}\,\tilde{s} > 0$ determine which roots $\kappa, \mu$ to keep in the analysis (to satisfy $\|u\| < \infty$) as well as the form of $\hat{u}_j, \hat{v}_j$ (distinct or multiple roots $\kappa, \mu$).

The main technical difficulty in the present application is the handling of any multiple roots $\kappa$ or $\mu$. The analysis will therefore be presented in two segments. First, the roots will be assumed to be distinct, and the stability criteria will be derived. Thereafter, the multiple roots will be found, and it will be verified that they do not alter the stability conclusion.

### 3.1. Preliminaries

We only consider schemes that are stable for the Cauchy problem (individually). Thus solutions to (7) must have $\mathrm{Re}\,\tilde{s} \leqslant 0$ for $\kappa = \exp(\mathrm{i}\theta)$, $\mu = \exp(\mathrm{i}\theta)$, $\theta \in [0, 2\pi)$. We consider schemes for which $\mathrm{Re}\,\tilde{s} < 0, \theta \neq 0$, to be *dissipative*, and schemes for which $\mathrm{Re}\,\tilde{s} = 0, \theta \in [0, 2\pi)$, to be *non-dissipative*. Note that stability of the Cauchy problems implies that there are no roots $\kappa$ or $\mu$ on the unit circle for $\mathrm{Re}\,\tilde{s} > 0$.

One useful and well-known result (cf. [6]) is the number of roots that satisfy $|\kappa|, |\mu| < 1$, i.e. $\|u\| < \infty$. Consider the characteristic equation (7a) for $\kappa$. Dividing by $\mathrm{Re}\,\tilde{s} > 0$ yields

$$\frac{\tilde{s}}{\mathrm{Re}\,\tilde{s}} = \sum_{k=-l_{\mathrm{I}}}^{0} \frac{a_k^{\mathrm{I}}}{\mathrm{Re}\,\tilde{s}} \kappa^k + \sum_{k=1}^{r_{\mathrm{I}}} \frac{a_k^{\mathrm{I}}}{\mathrm{Re}\,\tilde{s}} \kappa^k = P^-(\kappa, \tilde{s}) + P^+(\kappa, \tilde{s}). \tag{8}$$

For roots satisfying $|\kappa| > 1$

$$|P^-(\kappa,\tilde{s})| \leqslant \sum_{k=-l_\mathrm{I}}^{0} \frac{|a_k^\mathrm{I}|}{\mathrm{Re}\,\tilde{s}}|\kappa|^k < \sum_{k=-l_\mathrm{I}}^{0} \frac{|a_k^\mathrm{I}|}{\mathrm{Re}\,\tilde{s}},$$

while $|\tilde{s}|/\mathrm{Re}\,\tilde{s} \geqslant 1$. Thus for any given set of coefficients $\{a_k^\mathrm{I}\}$, $P^- \to 0$ as $\mathrm{Re}\,\tilde{s} \to \infty$, and (8) then has exactly $r_\mathrm{I}$ roots outside the unit circle in this limit. Since the roots are continuous functions of $\tilde{s}$, and since there are no roots on the unit circle for $\mathrm{Re}\,\tilde{s} > 0$, this implies that (7a) has $r_\mathrm{I}$ roots outside the unit circle for any $\tilde{s}$ with $Re\,\tilde{s} > 0$. Consequently, there are $l_\mathrm{I}$ roots inside the unit circle. Similarly, there are $l_\mathrm{II}$ roots of (7b) with $|\mu| < 1$. Note that the total number of roots equals the number of boundary conditions (4). Note also that $\kappa = 0$ is not a root, since if $l_\mathrm{I} = 0$ there are no roots inside the unit circle, and if $l_\mathrm{I} > 0$ then (7a) shows that $\kappa = 0$ is not a solution for any fixed $\tilde{s}$. Similarly, $\mu = 0$ is not a root.

Finally, we point out that the fact that there are $l_\mathrm{I}, l_\mathrm{II}$ roots inside the unit circle implies that schemes with $l_\mathrm{I}, l_\mathrm{II} \leqslant 1$ must necessarily have only distinct roots.

### 3.2. Distinct roots

For values of $\tilde{s}$ where the characteristic equations (7) have distinct roots, the solutions can be written as:

$$\hat{u}_j = \sum_{m=1}^{l_\mathrm{I}} \sigma_m \kappa_m^{j+l_\mathrm{I}},$$
$$\hat{v}_j = -\sum_{m=1}^{l_\mathrm{II}} \tau_m \mu^{j-l_\mathrm{I}},$$

where $\sigma_m$ and $\tau_m$ are some constants. Inserting this into the boundary conditions $\hat{u}_j - \hat{v}_{-j} = 0, j = -l_\mathrm{I}, \ldots, l_\mathrm{II} - 1$, yields

$$\sum_{m=1}^{l_\mathrm{I}} \sigma_m \kappa_m^{j+l_\mathrm{I}} + \sum_{m=1}^{l_\mathrm{II}} \tau_m \mu^{-j-l_\mathrm{I}} = 0, \quad j = -l_\mathrm{I}, \ldots, l_\mathrm{II} - 1,$$

which can be written on matrix form $J\rho = 0$ with $\rho = (\sigma_1, \ldots, \sigma_{l_\mathrm{I}}, \tau_1, \ldots, \tau_{l_\mathrm{II}})$ and

$$J = \begin{pmatrix} 1 & \ldots & 1 & 1 & \ldots & 1 \\ \kappa_1 & \ldots & \kappa_{l_\mathrm{I}} & \mu_1^{-1} & \ldots & \mu_{l_\mathrm{II}}^{-1} \\ \vdots & & & & & \vdots \\ \kappa_1^{l_\mathrm{I}+l_\mathrm{II}-1} & & & & & \mu_{l_\mathrm{II}}^{-l_\mathrm{I}-l_\mathrm{II}+1} \end{pmatrix}.$$

This is a van der Monde matrix with determinant

$$\det J = \prod_{i<j}(\eta_i - \eta_j), \quad \eta_i = \begin{cases} \kappa_i, & i \leqslant l_\mathrm{I}. \\ \mu_{i-l_\mathrm{I}}^{-1}, & i > l_\mathrm{I}. \end{cases}$$

Since the roots are distinct, there is a non-trivial solution only if $\kappa_i = \mu_j^{-1}$ for some $i$ and $j$. The requirement of a finite solution $\|u\| < \infty$ for $\mathrm{Re}\,\tilde{s} > 0$ implies that $|\kappa|, |\mu| < 1$, and hence there is no non-trivial solution with distinct roots for $\mathrm{Re}\,\tilde{s} > 0$, and the Godunov–Ryabenkii condition (which is necessary for stability, cf. [6]) is satisfied for the distinct roots (it remains to be verified that it still holds when the multiple roots are taken into account).

The sufficient condition for stability (the Kreiss condition) is that $\det J \neq 0$ holds for $\mathrm{Re}\,\tilde{s} = 0$. To find any possible roots that would yield $\det J = 0$, suppose $\kappa = \mu^{-1} = \exp(\mathrm{i}\theta)$, $\theta \in [0, 2\pi)$, and $\mathrm{Re}\,\tilde{s} = 0$. Note that this supposition includes roots approaching the unit circle both from the inside and outside. Inserting into the characteristic equations (7) yields

$$\sum_{k=-l_{\mathrm{I}}}^{r_{\mathrm{I}}} a_k^{\mathrm{I}} \cos(k\theta) = 0, \tag{9a}$$

$$\sum_{k=-l_{\mathrm{II}}}^{r_{\mathrm{II}}} a_k^{\mathrm{II}} \cos(k\theta) = 0, \tag{9b}$$

$$\sum_{k=-l_{\mathrm{I}}}^{r_{\mathrm{I}}} a_k^{\mathrm{I}} \sin(k\theta) - \sum_{k=-l_{\mathrm{II}}}^{r_{\mathrm{II}}} a_k^{\mathrm{II}} \sin(k\theta) = 0, \tag{9c}$$

where the real and imaginary parts have been separated. We must now eliminate those roots $\kappa$ and $\mu$ that approached from outside the unit circle. How a root approached the unit circle can be determined by considering the small perturbations $\tilde{s} + \delta$, $(1 + \varepsilon_\kappa)\kappa$, and $(1 + \varepsilon_\mu)\mu$, for real $\delta > 0$. Note that $\kappa$ and $\mu$ are the roots corresponding to $\delta = 0$, and that only roots $\kappa$ for which $\varepsilon_\kappa < 0$ and $\mu$ for which $\varepsilon_\mu < 0$ should be included in the analysis. With the Taylor expansion $(1 + \varepsilon)^k \approx 1 + k\varepsilon$ this yields

$$0 < \delta \approx -\tilde{s} + \sum_{k=-l_{\mathrm{I}}}^{r_{\mathrm{I}}} a_k^{\mathrm{I}}(1 + k\varepsilon_\kappa)\kappa^k = \varepsilon_\kappa \sum_{k=-l_{\mathrm{I}}}^{r_{\mathrm{I}}} k a_k^{\mathrm{I}} \mathrm{e}^{\mathrm{i}k\theta}, \tag{10a}$$

$$0 < \delta \approx -\tilde{s} - \sum_{k=-l_{\mathrm{II}}}^{r_{\mathrm{II}}} a_k^{\mathrm{II}}(1 + k\varepsilon_\mu)\mu^k = -\varepsilon_\mu \sum_{k=-l_{\mathrm{II}}}^{r_{\mathrm{II}}} k a_k^{\mathrm{II}} \mathrm{e}^{-\mathrm{i}k\theta}. \tag{10b}$$

We now note the following, pending investigation of any multiple roots:

(1) $\theta = 0$, i.e. $\kappa = \mu = 1$, $\tilde{s} = 0$, is always a solution of (9) due to the first consistency requirement (5a). The second consistency requirement (5b) together with (10a) shows that $\kappa$ always approaches from outside the unit circle. Later it will be shown that $\theta = 0$ is always a distinct root, and hence this root does not cause instability.

(2) If either scheme is dissipative such that $\mathrm{Re}\,\tilde{s} < 0$ for $\theta \neq 0$, then there are no other roots, and the Kreiss condition is satisfied (pending any multiple roots). Schemes with $l_{\mathrm{I}}, l_{\mathrm{II}} \leqslant 1$ have no multiple roots, and thus they are stable when coupled if at least one scheme is dissipative. This proves stability for the simple example in Section 2.1, and extends the result of Ciment [9] who proved stability for the case of both schemes being dissipative.

(3) If both schemes are non-dissipative, then (9a) and (9b) are satisfied for all $\theta \in [0, 2\pi)$. Orthogonality of the trigonometric functions implies that $a_k^{\mathrm{I,II}} = -a_{-k}^{\mathrm{I,II}}$, i.e. that both schemes are centered and anti-symmetric. For such schemes, (10) yields

$$\begin{aligned} \delta &\approx 2\varepsilon_\kappa \sum_{k=1}^{r_{\mathrm{I}}} k a_k^{\mathrm{I}} \cos(k\theta), \\ \delta &\approx -2\varepsilon_\mu \sum_{k=1}^{r_{\mathrm{II}}} k a_k^{\mathrm{II}} \cos(k\theta). \end{aligned} \tag{11}$$

For this situation, (9c) must be solved for the specific schemes in question to find all roots $\theta$. For each such root, (11) must then be evaluated to verify that at least one of $\kappa$ or $\mu$ approaches the unit circle from the outside and thus can be discarded.

(4) The direction of the coupling may affect the stability for two non-dissipative schemes. Eqs. (9) are all invariant under the transformation $a_k^{\mathrm{I}} \to -a_{-k}^{\mathrm{II}}$, $a_k^{\mathrm{II}} \to -a_{-k}^{\mathrm{I}}$, which implies that the roots $\theta$ are unchanged. If there exists a root $\theta$ for which $\varepsilon_\kappa$ and $\varepsilon_\mu$ have the same sign, then the hybrid method is only stable when coupled in the direction for which both roots approach from outside the unit circle.

At this stage, before having considered any multiple roots, there are essentially two situations. First, if at least one of the schemes is dissipative then the Kreiss condition is guaranteed to be satisfied. This is likely the most natural situation in hybrid methods for shock/turbulence interactions, where many popular nonlinear shock-capturing schemes (like ENO and WENO) are designed to become upwind-biased in response to features

in the solution. In fact, the standard ENO/WENO schemes are upwind-biased even in their optimal stencils. The second situation is that of neither scheme being dissipative, and thus both being centered and anti-symmetric. One case where this could happen is where schemes of different accuracy are used in different parts of the domain. In this case there is no guarantee that the Kreiss condition is satisfied, and one must verify that there are no roots $\kappa = \mu^{-1}$ for which both $\kappa$ and $\mu$ approach from inside the unit circle.

### 3.3. Multiple roots

For the distinct roots the solutions $\hat{u}_j$ and $\hat{v}_j$ are of a form that yields a van der Monde matrix with a particularly suitable expression for the determinant, and this fact greatly simplified the analysis for that case. For values of $\tilde{s}$ that yield multiple roots $\kappa$ and/or $\mu$, one or both of $\hat{u}_j$ and $\hat{v}_j$ takes a different form which does not yield a van der Monde matrix. Thus a general analysis is difficult for this case, and one must resort to verifying $\det J \neq 0$ by setting up a suitable form of the solution and computing the determinant. This only needs to be done for a limited number of multiple roots, and hence the added work is not excessive in practice.

To find all multiple roots, first multiply the characteristic equation (7a) by $\kappa^{l_\mathrm{I}}$ and take the derivative with respect to $\kappa$ as

$$\tilde{s}\kappa^{l_\mathrm{I}} = \sum_{k=-l_\mathrm{I}}^{r_\mathrm{I}} a_k^\mathrm{I} \kappa^{k+l_\mathrm{I}},$$

$$l_\mathrm{I}\tilde{s}\kappa^{l_\mathrm{I}-1} = \sum_{k=-l_\mathrm{I}+1}^{r_\mathrm{I}} (k+l_\mathrm{I}) a_k^\mathrm{I} \kappa^{k+l_\mathrm{I}-1}.$$

For fixed $\tilde{s}$, any multiple root $\kappa$ must satisfy both these equations. Eliminating $\tilde{s}$ and repeating for $\mu$ yields the equations for the multiple roots for all $\tilde{s}$

$$\sum_{k=-l_\mathrm{I}}^{r_\mathrm{I}} k a_k^\mathrm{I} \kappa^{k+l_\mathrm{I}} = 0, \tag{12a}$$

$$\sum_{k=-l_\mathrm{II}}^{r_\mathrm{II}} k a_k^\mathrm{II} \mu^{k+l_\mathrm{II}} = 0. \tag{12b}$$

These equations are to be considered for $\mathrm{Re}\,\tilde{s} \geqslant 0$. Note that, if $\mathrm{Re}\,\tilde{s} = 0$ and $|\kappa| = 1$, then $\hat{u}_j$ should only have a different form if more than one of the multiple roots approached the unit circle from the inside (and similarly for $\mu$ and $\hat{v}_j$).

Below are three examples which illustrate the application of the Kreiss theory. Special attention is paid to the handling of the multiple roots.

### 3.4. Example 1: coupled central 2nd and 4th order schemes

Consider the case with $a_1^\mathrm{I} = 1/2$, $(a_1^\mathrm{II}, a_2^\mathrm{II}) = (2/3, -1/12)$ and $a_k^\mathrm{I,II} = -a_{-k}^\mathrm{I,II}$, i.e. a region with a 2nd order central scheme coupled to a region with a 4th order central scheme. First we consider the distinct roots. Eq. (9c) has the solutions $\theta = 0, \pi$. The first one has already been covered, and for the second one we have $\kappa = \mu = -1$. Inserting into the perturbations (11) yields $\varepsilon_\kappa \approx -\delta < 0$ and $\varepsilon_\mu \approx 3/5\delta > 0$. Thus $\mu$ approaches from the outside and can be discarded.

Now consider the multiple roots. For $\kappa$, we know that there are no multiple roots since only $l_\mathrm{I} = 1$ roots reside inside the unit circle for $\mathrm{Re}\,\tilde{s} > 0$. For $\mu$, (12b) yields multiple roots $\mu \approx 4.2121, -0.2247 \pm 0.9744i$, 0.2374, with associated $\tilde{s} \approx -1.1760, \mp 1.3722i$, 1.1760. The first is outside the unit circle and can be discarded. The next two have $\mathrm{Re}\,\tilde{s} = 0$, and thus we perturb as $\tilde{s} + \delta$ and solve the characteristic equation (7b) for the displaced roots. The perturbation causes each double root to separate into two distinct roots, with one going outside the unit circle, and thus the proper form of the solution is not altered. The final multiple root

$\mu \approx 0.2374$ is inside the unit circle and $\mathrm{Re}\,\tilde{s} > 0$. Thus we need to set up a different form of the solution for this value of $\tilde{s} \approx 1.1760$ as

$$\hat{v}_j = -\tau_1 \mu^{j-l_\mathrm{I}} - \tau_2(-j + l_\mathrm{I} + 1)\mu^{j-l_\mathrm{I}},$$

which yields a boundary condition matrix

$$J = \begin{pmatrix} 1 & 1 & 1 \\ \kappa & \mu^{-1} & 2\mu^{-1} \\ \kappa^2 & \mu^{-2} & 3\mu^{-2} \end{pmatrix},$$

where $\kappa \approx -0.3677$ from (7a). Evaluating the determinant yields $\det J \neq 0$, and thus this multiple root does not cause instability. Overall, we conclude that the Kreiss condition is satisfied and that the coupled scheme is stable.

This example shows the typical application of the stability analysis, in that the half-plane $\mathrm{Re}\,\tilde{s} \geqslant 0$ is first covered by supposing the roots to be distinct, and then a few multiple roots are considered to verify that they do not alter the analysis. Note that the perturbation analysis is different in the two cases: for the distinct roots it is a matter of determining whether the root should be included in the analysis at all, whereas for the multiple roots it is a matter of determining whether a different form of the solution is needed.

We also note that (9c) is in fact a relation between the modified wavenumbers of the different schemes. The exact derivative of a function $u_j = \exp(\mathrm{i}kx_j)$ is $\mathrm{i}ku_j$. Analogously, the difference approximation of the derivative is $\mathrm{i}k'u_j$, where $k'$ is the modified wavenumber. Introducing the notation $\Theta = k'h$, this is defined for anti-symmetric schemes as

$$\Theta^{\mathrm{I,II}}(\theta) = 2\sum_{k=1}^{r_{\mathrm{I,II}}} a_k^{\mathrm{I,II}} \sin(k\theta). \tag{13}$$

Thus Eq. (9c) can be written as

$$\Theta^{\mathrm{I}}(\theta) = \Theta^{\mathrm{II}}(\theta)$$

for non-dissipative schemes, with roots $\theta$ where the modified wavenumbers are equal. Many standard central schemes of different order have everywhere different modified wavenumbers, and therefore no roots other than $\theta = 0, \pi$, where it must be verified whether the $\theta = \pi$ root is permissible or not. When coupling non-standard central schemes, e.g. those where the coefficients are determined by some optimization criterion, there may be additional roots $\theta$ that need investigation.

The connection with the modified wavenumber was noted by Trefethen [10], who interpreted the Kreiss theory in terms of the group velocity of the difference scheme near the boundary. The group velocities with the present notation are

$$v_\mathrm{g}^{\mathrm{I}} = -\frac{\mathrm{d}\Theta^{\mathrm{I}}}{\mathrm{d}\theta},$$
$$v_\mathrm{g}^{\mathrm{II}} = \frac{\mathrm{d}\Theta^{\mathrm{II}}}{\mathrm{d}\theta}.$$

Taking the derivative of (13) yields

$$v_\mathrm{g}^{\mathrm{I}} = -2\sum_{k=1}^{r_\mathrm{I}} k a_k^{\mathrm{I}} \cos(k\theta) \approx -\frac{\delta}{\varepsilon_\kappa},$$
$$v_\mathrm{g}^{\mathrm{II}} = 2\sum_{k=1}^{r_\mathrm{II}} k a_k^{\mathrm{II}} \cos(k\theta) \approx -\frac{\delta}{\varepsilon_\mu},$$

where the relation to the perturbations stems from (11). Therefore a positive group velocity implies that the corresponding root approached the unit circle from the inside. The next example brings out this connection more clearly.

### 3.5. Example 2: coupled central schemes with stability in only one direction

Consider the coupling of the standard 8th order central scheme given by $(a_1^{\mathrm{I}}, a_2^{\mathrm{I}}, a_3^{\mathrm{I}}, a_4^{\mathrm{I}}) = (4/5, -1/5, 4/105, -1/280)$ to the 'optimized' scheme $(a_1^{\mathrm{II}}, a_2^{\mathrm{II}}) = (0.81, -0.155)$, and $a_k^{\mathrm{I,II}} = -a_{-k}^{\mathrm{I,II}}$. The second scheme here is not standard, but representative of schemes where the coefficients are chosen partly to increase the range of resolved wavenumbers. While the coefficients used here are chosen to illustrate an aspect of stability, we note that optimized schemes are popular in several areas, including acoustic wave propagation and large eddy simulation. Note that the scheme is consistent and second order accurate.

The modified wavenumbers given by (13) for the two schemes are shown in Fig. 2. We first note that the optimized scheme used here is by no means unreasonable, in fact its modified wavenumber is somewhat similar to the 8th order scheme with better resolution of the medium wavelength modes than the standard 4th order central scheme (not shown). The figure shows that the modified wavenumbers are equal for $\theta = 0, \theta_r, \pi$, where $\theta_r \approx 1.938$. Thus these are the roots of (9c), along with $-\theta_r$ by anti-symmetry. The perturbations (11) become $\delta/\varepsilon_\kappa \approx (0.22, -2.7, 0.22)$ and $\delta/\varepsilon_\mu \approx (0.12, 2.2, 0.12)$ for $(\theta_r, \pi, -\theta_r)$. Thus the $\mu$ roots approach from the outside and can be discarded, and the scheme is stable pending investigation of the multiple roots.

Solving (12) yields two multiple roots $\kappa$ on the unit circle, two multiple roots $\mu$ on the unit circle, and one multiple root $\mu \approx 0.3466$ with $\tilde{s} \approx 0.7846$. All four roots on the unit circle separate in/outside when perturbed, but the final root needs to be considered. Solving (7a) for this $\tilde{s}$ yields $(\kappa_1, \kappa_2, \kappa_{3,4}) \approx (-0.7524, 0.1314, 0.0513 \pm 0.1591i)$. Thus we set up a new form of the solution $\hat{v}_j$ as above and find the boundary condition matrix

$$J = \begin{pmatrix} 1 & 1 & 1 & 1 & 1 & 1 \\ \kappa_1 & \kappa_2 & \kappa_3 & \kappa_4 & \mu^{-1} & 2\mu^{-1} \\ \kappa_1^2 & \kappa_2^2 & \kappa_3^2 & \kappa_4^2 & \mu^{-2} & 3\mu^{-2} \\ \kappa_1^3 & \kappa_2^3 & \kappa_3^3 & \kappa_4^3 & \mu^{-3} & 4\mu^{-3} \\ \kappa_1^4 & \kappa_2^4 & \kappa_3^4 & \kappa_4^4 & \mu^{-4} & 5\mu^{-4} \\ \kappa_1^5 & \kappa_2^5 & \kappa_3^5 & \kappa_4^5 & \mu^{-5} & 6\mu^{-5} \end{pmatrix}. \tag{14}$$

This determinant is non-zero, and thus this multiple root does not cause instability. We then conclude that the hybrid scheme is stable when coupled in the direction 8th order → optimized scheme. Note that the direction of the coupling is defined here in relation to the direction of propagation in the model problem (1).

Now consider the opposite direction of coupling, i.e. let $a_k^{\mathrm{I}} \to -a_{-k}^{\mathrm{II}}$ and $a_k^{\mathrm{II}} \to -a_{-k}^{\mathrm{I}}$. The perturbations then become $\delta/\varepsilon_\kappa \approx (-0.12, -2.2, -0.12)$ and $\delta/\varepsilon_\mu \approx (-0.22, 2.7, -0.22)$ for $(\theta_r, \pi, -\theta_r)$. Thus the roots $\pm\theta_r$ approach from inside the unit circle, and the coupled scheme is unstable in this direction of coupling, i.e.

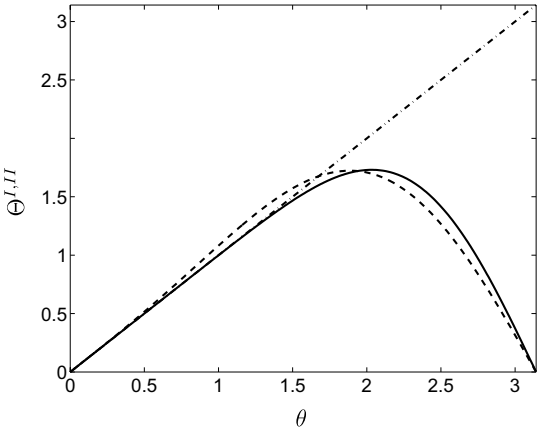


Fig. 2. Modified wavenumbers for the two schemes in Section 3.5. Standard 8th order (solid), optimized (dashed), and exact (dash-dotted).

for optimized → 8th order scheme. There is then no need to check the multiple roots (although none satisfies the boundary condition, and thus does not cause instability).

To illustrate this situation, the model problem (1) is solved on a domain $x \in [0,1]$ with $N+1$ points and grid spacing $h = 1/N$. The interface is located at $x_{\text{int}} = 0.7$, and the initial condition is taken as

$$u_j(0) = R_j \exp\left(-6\left(\frac{x_j - x_{\text{int}}}{5h}\right)^2\right), \quad j = 0, \pm 1, \pm 2, \ldots, \tag{15}$$

where $u_j$ is defined in analogy with (2) and $R_j \in (-1,1)$ is a uniformly distributed random number. This initial condition excites all modes and is highly localized around the interface. The solution is integrated in time using the trapezoidal rule with a time step small enough such that the temporal discretization has negligible effect on the solution (CFL number of 0.05). To approximate a Cauchy problem, the temporal integration is halted when the solution near the boundaries becomes larger than $10^{-8}$ in magnitude.

Fig. 3(a) shows the growth of the solution norms for both the stable (8th order → optimized) and unstable (optimized → 8th order) configurations. The growth for the unstable configuration increases as the grid is refined, in fact the curves collapse if plotted versus $t/h$ instead (not shown). The growth approximately proportional to $t/h$ shows that the scheme is unstable, and hence the numerical experiment confirms the theory. The stable configuration yields a roughly constant norm and is stable, as predicted by the theory.

One note on the initial condition is in order. Since the unstable mode is known in this case, this mode could have been used as the initial condition instead. Doing so results in qualitatively similar results, albeit with larger values for $\|u\|$. The random initial condition was used here to excite all possible modes.

The solutions after a long time on the finest grid are shown in Fig. 3(b). While both solutions are highly inaccurate with large spreading of numerical noise in both directions, the figure still shows the essential difference between the two coupling configurations. The stable configuration shows the noise propagating away from the interface at the wavenumber-dependent group velocity of the schemes, but there is little or no generation of new noise around the interface. The unstable configuration, on the other hand, displays continuous generation of energy around the interface, leading to a growing norm.

At this point we recall Trefethen's [10] interpretation of the Kreiss theory in terms of the numerical group velocity discussed above. The modified wavenumbers $\Theta^{\text{I,II}}$ in Fig. 2 of the different schemes have opposite slopes at the point $(\theta_r)$ where they intersect, which then implies that both the group velocities $v_g^{\text{I,II}}$ and the perturbations $\varepsilon_\kappa, \varepsilon_\mu$ have the same signs for that wavenumber. The unstable configuration is that for which the roots approach from the inside and therefore $v_g^{\text{I,II}} > 0$. This enables transport of any energy generated at the interface into the rest of the domain.

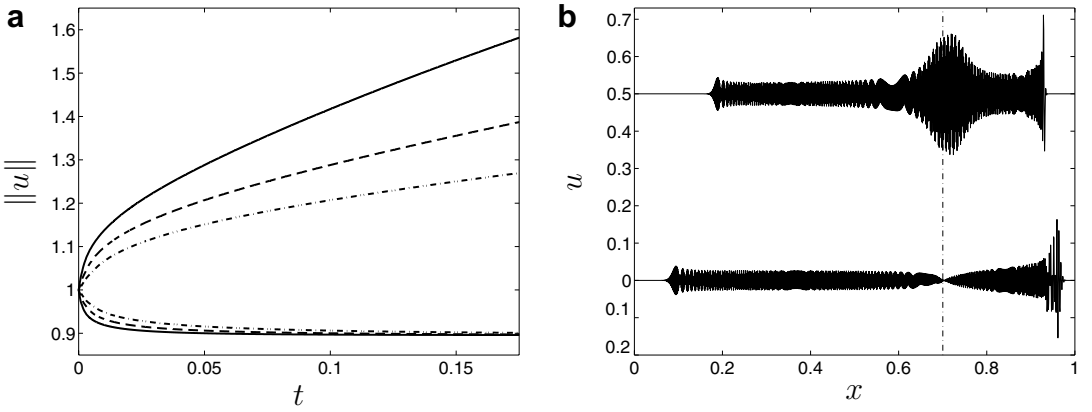


Fig. 3. Evolution of the norm and the solution after long time for the example in Section 3.5. (a) Norms for stable (lower curves) and unstable (upper) coupling directions for grid sizes $N = 400$ (dash-dotted), $N = 800$ (dashed), and $N = 1600$ (solid). (b) Solutions after long time for stable (lower) and unstable (upper, offset by 0.5) coupling directions for finest grid. The dash-dotted line marks the interface.

### 3.6. Example 3: coupled identical schemes

As a final example we consider the special case of coupling identical non-dissipative schemes. While artificial, this special case illustrates some of the subtleties in the Kreiss theory.

Consider $a_1^{\mathrm{I}} = a_1^{\mathrm{II}} = 1/2$ and $a_k^{\mathrm{I,II}} = -a_{-k}^{\mathrm{I,II}}$. Thus the coupled problem is really just a standard Cauchy problem, and we know that it is stable. Following instead the analysis of the Kreiss theory, we first note that there are no multiple roots since $l_{\mathrm{I,II}} = 1$. For the distinct roots, every $\theta \in [0, 2\pi)$ solves (9). The perturbations (11) become

$$\delta \approx \varepsilon_\kappa \cos\theta,$$
$$\delta \approx -\varepsilon_\mu \cos\theta.$$

Thus the roots approach from different sides for $\theta \neq \pi/2, 3\pi/2$, but for those two values the first order perturbation is insufficient. A more careful calculation shows that it is possible to perturb the roots such that both approach from inside the unit circle as $\mathrm{Re}\,\tilde{s} \to 0^+$. This implies that these roots correspond to generalized eigenvalues for $\mathrm{Re}\,\tilde{s} = 0$, and thus that the Kreiss condition is not satisfied – but we know that the scheme is stable by considering the case as a Cauchy problem.

The Kreiss condition is thus a little too strong for this special case. The Kreiss condition guarantees that an estimate of the solution is obtained in terms of arbitrary but bounded boundary data $g(t)$. If one of the conditions in (4) is modified to $u_j^{\mathrm{I}} = u_{-j}^{\mathrm{II}} + g(t)$, we can rewrite it as an extra forcing term proportional to $g(t)/h$ in the original difference scheme, and an estimate in terms of $|g(t)|$ should not be expected. Trefethen [10] considered a similar special case which is stable in the $l_2$-norm yet does not satisfy the Kreiss condition. A thorough discussion along with a different example is given in section 12.5 of [6].

### 3.7. Solution bound

Having found the conditions for which the Kreiss condition is satisfied, the Kreiss theory provides bounds on the solution that prove stability. There are two cases.

If neither scheme is dissipative, then $l_{\mathrm{I}} = r_{\mathrm{I}}$, $l_{\mathrm{II}} = r_{\mathrm{II}}$, and both schemes are semibounded for the individual Cauchy problems (by their anti-symmetry). Then Theorem 12.2.3 of [6] asserts that the approximation is strongly stable, i.e. that, for smooth initial data

$$\|u(t)\| \leqslant Ke^{\alpha t}\|u(0)\|,$$

where the discrete solution $u_j$ is defined in analogy with (2).

If either scheme is dissipative, then (without the requirements of semiboundedness and the conditions on $l_{\mathrm{I,II}}$ and $r_{\mathrm{I,II}}$) Theorem 12.4.4 of [6] asserts that the approximation is strongly stable in the generalized sense, i.e. that, for smooth initial data,

$$\int_0^\infty \mathrm{e}^{-\eta t}\|u(t)\|\mathrm{d}t \leqslant K(\eta)\|u(0)\|,$$

for all $\eta > \eta_0$, and $K(\eta) \to 0$ as $\eta \to \infty$.

### 3.8. Application to a nonlinear problem

The analysis presented here is restricted to linear problems and schemes, but many applications of scientific interest are nonlinear both in the underlying PDE and the numerical method. One commonly used test problem is the one-dimensional shock/entropy interaction problem devised by Shu and Osher [1]. The Euler equations for a perfect gas with gas constant $\gamma = 1.4$ are solved on a domain $x \in [-5, 5]$ using a uniform grid with spacing $h = 10/200$. The initial condition is

$$(\rho, u, p) = \begin{cases} (3.857, 2.629, 10.333), & x < -4, \\ (1 + 0.2\sin(5x), 0, 1), & x \geqslant -4, \end{cases}$$

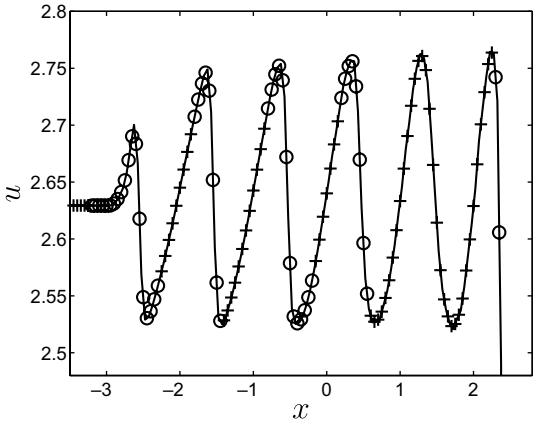


Fig. 4. Instantaneous velocity (solid) for a train of moving shocks. Hybrid WENO/central difference algorithm, where circles denote points treated by WENO and crosses denote points treated by the central scheme.

where $(\rho, u, p)$ are the density, velocity, and pressure, respectively. From this initial condition, the main shock travels to the right and interacts with the density field. This generates acoustic and entropy waves, where the acoustic waves steepen into weaker shocks as time progresses. A hybrid method which uses an 8th order central scheme away from the shocks and a 7th order WENO scheme [11] around the shocks is used. A solution-adaptive sensor taken from [4] is used to find those grid points where the WENO scheme should be applied.

Applying the Kreiss theory to this problem amounts to finding multiple roots, since the WENO scheme is dissipative in its linearized stencil. There are only three multiple roots in each coupling direction, and none yield a singular determinant. Thus the hybrid method is linearly stable.

The solution at $t = 1.8$ is shown in Fig. 4, at which time there are five regions of WENO points, and hence ten interfaces where the schemes are coupled. Despite the strongly nonlinear nature of the problem, the rather low resolution, and the frequent switching between the different schemes, no noise around the interfaces is visible. This suggests that the stability characteristics may carry over to nonlinear problems as well.

## 4. Summary and discussion

The case of hybrid finite difference methods, where different schemes are applied in different regions of the domain, is investigated from a stability perspective. The Kreiss theory [5,6] is used to analyze stability for general linear schemes of arbitrary order and stencil size. The analysis consists of two separate parts, where a limited number of potential multiple roots must be examined individually, whereas the remainder of the half-plane $\mathrm{Re}\,\tilde{s} \geqslant 0$ can be handled by finding points where the modified wavenumbers of the two schemes are equal. Since schemes with $l_{\mathrm{I,II}} \leqslant 1$, i.e. with only one point extending across the interface, can not have any multiple roots, the different cases discussed in Section 3.2 become sufficient conditions for stability.

The only assumptions involved are that both schemes are consistent and stable for the Cauchy problem (individually). An example involving an 'optimized' scheme is shown to be stable only for one coupling direction, thus showing that the issue of stability for hybrid difference methods is non-trivial and can not be taken for granted.

It is also shown that the energy method with the most natural norm does not prove stability for the coupled problem. While there may exist norms for which an energy estimate could be found, this was not pursued here. The result from the analysis with the energy method is interesting in the context of numerical noise around the interface. Even stable methods may generate transient growth of disturbances, and thus the appearance of numerical noise around the interface seen and/or discussed in [2–4] is not surprising. The present stability proof shows that, for linearized problems, the numerical noise is transient and does not affect the stability.

## Acknowledgment

Financial support has been provided by the DoE Scientific Discovery through Advanced Computing (SciDAC) program. The first author also gratefully acknowledges additional support from the Natural Sciences and Engineering Research Council of Canada.

## References

[1] C.-W. Shu, S.J. Osher, Efficient implementation of essentially nonoscillatory shock capturing schemes II, J. Comput. Phys. 83 (1989) 32–78.
[2] N.A. Adams, K. Shariff, A high-resolution hybrid compact-ENO scheme for shock–turbulence interaction problems, J. Comput. Phys. 127 (1996) 27–51.
[3] Y.-X. Ren, M. Liu, H. Zhang, A characteristic-wise hybrid compact-WENO scheme for solving hyperbolic conservation laws, J. Comput. Phys. 192 (2003) 365–386.
[4] D.J. Hill, D.I. Pullin, Hybrid tuned center-difference-WENO method for large eddy simulation in the presence of strong shocks, J. Comput. Phys. 194 (2004) 435–450.
[5] B. Gustafsson, H.-O. Kreiss, A. Sundström, Stability theory of difference approximations for mixed initial boundary value problems II, Math. Comput. 26 (119) (1972) 649–686.
[6] B. Gustafsson, H.-O. Kreiss, J. Oliger, Time Dependent Problems and Difference Methods, John Wiley & Sons, 1995.
[7] J.C. Strikwerda, Initial boundary value problems for the method of lines, J. Comput. Phys. 34 (1980) 94–107.
[8] M. Goldberg, E. Tadmor, Scheme-independent stability criteria for difference approximations of hyperbolic initial-boundary value problems II, Math. Comput. 36 (154) (1981).
[9] M. Ciment, Stable matching of difference schemes, SIAM J. Numer. Anal. 9 (4) (1972) 695–701.
[10] L.N. Trefethen, Instability of difference models for hyperbolic initial boundary value problems, Commun. Pure Appl. Math. 37 (1984) 329–367.
[11] G.-S. Jiang, C.-W. Shu, Efficient implementation of weighted ENO schemes, J. Comput. Phys. 126 (1996) 202–228.